Application of natural adsorbent from silver impregnated *Arachis hypogaea* based thereon in the processes of hexavalent chromium for the purification of water

Shashi Prabha Dubey, Krishna Gopal*

Aquatic Toxicology Division, Indian Institute of Toxicology Reseach (CSIR), M.G. Marg, P.O.Box 80, Lucknow - 226001, UP, India

ABSTRACT

Different industries generate huge amounts of chromium, both in solid and liquid form which leached out and find their way to the aquifers. Here we report the removal of Cr(VI) by the silver impregnated activated carbon developed from agricultural waste material at pH 3 from drinking water. Result revealed that adsorption of chromium(VI) on silver impregnated groundnut husk carbon was endothermic in nature. Thermodynamic parameters such as the entropy change, enthalpy change and Gibbs free energy change were found to be $1.68\,kJ\,mol^{-1}\,K^{-1}$, $0.46\,kJ\,mol^{-1}$ and $-4.38\,kJ\,mol^{-1}$, respectively. The measured adsorption kinetics is well described by a pseudo first-order kinetic model. The effect of flow rate, column depth and initial concentration of chromium(VI) on the removal of chromium by the impregnated adsorbent is presented. Scanning Electron Microscope (SEM), Electron Dispersive X-ray Analysis (EDX) and FTIR analysis show that the silver is impregnated on the surface. Shifts in the FTIR spectra suggest that dichromate binding occurs with silver and other functional groups and that silver treated groundnut husk carbon removes chromium. The 96 h static acute toxicity test was conducted to ensure the safe disposal of the used adsorbent.

1. Introduction

Industrial and mining wastewaters are important sources of pollution of heavy metals [1]. Chromium is used widespreadly and it engendered a serious pollutant of water [2]. The use of chromate and dichromate in metal plating and as corrosion control agents in cooling waters is quite extensive. It is well-known that Cr(VI) is toxic to living systems and must be removed from wastewater before it can be discharged [3]. Chromium-plating processes are the main source of Cr(VI) pollution. Cr(VI) is a skin and mucous membrane irritant and some of these hexavalent compounds produce an allergic contact dermatitis characterized by eczema [4,5]; it is also recognized as a pulmonary carcinogen [4,6]. The maximum concentration limit for Cr(VI) for discharge into inland surface waters is 0.1 mg/L and in potable water is 0.05 mg/L [7].

The remediation of Cr(VI) contaminated industrial samples is gaining great interest due to limitations in potable water supplies. The main strategies for Cr(VI) removal from wastewaters are precipitation as $Cr(OH)_3$ [8] and ion exchange [9]. In addition, there are other options such as membrane filtration [10] and reduction [11,12], electrochemical precipitation [13], ion exchange [14], ultra filtration [15] and reverse osmosis [16].

Among the naturally available products, herbs, geochemicals/minerals as well as industrial/domestic by products, some have been found to contain considerable potential for purification and disinfection of water [17]. A variety of natural adsorbent, indigenous minerals and synthetic adsorbents are known which can be used to remove chromium from drinking water. As one of the most promising techniques for removal of chromium from industrial wastewaters, adsorption technology has been employed for many years and the effectiveness of various adsorbents has been demonstrated [18].

There are several adsorbents mentioned which can remove chromium from drinking water, viz. hazelnut shell carbon [19], coconut shell charcoal and commercial activated carbon modified with oxidizing agents and/or chitosan [20], activated rice husk carbon and activated alumina for chromium [21], *Rizopus nigricans* [22], chemically treated biomass of Ecklonia species [23], biological wastes and vermiculite [24], chitosan coated acid treated oil palm shell charcoal [25], Powder carbon [26], eucalyptus bark [27] and synthetic adsorbents [28] have been reported in the literature.

Groundnut has enormous amount of agricultural waste. Preliminary studies have shown that it is feasible to prepare chars with

* Corresponding author. Tel.: +91 522 2220207/2227586x259/260; fax: +91 522 2628227.
E-mail address: krishnagopaldubey@gmail.com (K. Gopal).

sufficient densities and high porosity from groundnut husk [29]. The exchange/sorption properties of groundnut husk are due to presence of some functional groups such as carboxylic, hydroxyl, etc., which have high affinity for metal ions [30]. The use of groundnut husk with surface modification by silver impregnation to improve its metal removal performance would add to its economic value [31].

2. Materials and methods

2.1. Materials

Chemicals used in the study were of analytical grade (Merck, Germany). Synthetic samples used in the study were prepared using double distilled deionized water. All the glasswares and sample bottles were soaked in hot water and rinsed with laboratory dish soap (Lavolene) for at least 2 h and then rinsed with deionized water. Hexavalent chromium Cr(VI) stock solution (1000 mg/L) was prepared by dissolving potassium dichromate in de-ionized water and stored in airtight polythene terphthalate (PET) bottles at a temperature less than 2 °C. Further working solutions were freshly prepared from stock solution for each experimental run. Concentration of Cr(VI) was measured by atomic absorption spectrophotometer.

2.2. Thermodynamics

In order to determine thermodynamic parameters, experiments were carried out at different temperatures in the range of 303–323 K for Cr(VI) adsorption. The thermodynamic parameters such as standard Gibb's free energy change ($\Delta G°$), enthalpy change ($\Delta H°$) and entropy change ($\Delta S°$) were estimated to evaluate the feasibility and nature of the adsorption process. The Gibb's free energy change, of the process is related to equilibrium constant by the equation

$$\Delta G° = -RT \ln K_c \tag{1}$$

where T is temperature in K, R is ideal gas constant having value as 8.314 J mol^{-1} K^{-1} and K_c is thermodynamic equilibrium constant.

The thermodynamic equilibrium constant, was determined as

$$K_c = \frac{C_a}{C_e} \tag{2}$$

where C_a is mg of adsorbent adsorbed per liter and C_e is the equilibrium concentration of solution, mg/L.

According to thermodynamics, the Gibb's free energy change is also related to the enthalpy change ($\Delta H°$) and entropy change ($\Delta S°$) at constant temperature by the following equation,

$$\Delta G° = \Delta H° - T\Delta S° \tag{3}$$

Now using Eqs. (3) and (1) can be transformed to Eq. (4)

$$\ln K_c = \frac{\Delta S°}{R} - \frac{\Delta H°}{RT} \tag{4}$$

The values of enthalpy change ($\Delta H°$) and entropy change ($\Delta S°$) were calculated from the slope and intercept of the plot of $\ln K_c$ versus, $1/T$ ($R^2 = 0.94$).

Silver impregnated groundnut husk carbon used for the removal of hexavalent chromium was prepared in the laboratory. The details of the adsorbent preparation and comparison of chromium removal efficiency with other adsorbents have been discussed elsewhere [31]. Adsorption studies in the temperature range 303–323 K were conducted to determine thermodynamics constants such as Gibbs free energy change ($\Delta G°$), enthalpy change ($\Delta H°$) and entropy change ($\Delta S°$) for the system and to ascertain the sorption mechanism. For this study, measured adsorbents were used for removal

of chromium Cr(VI) in a conical flask and allowed to equilibrate for optimum time period at the different temperatures ranging from 303 K to 323 K. Residual chromium concentrations determined in each sample after equilibrium was attained.

2.3. Kinetic studies

A number of stoppered flasks (100 mL) containing different concentrated solution of chromium(VI) was agitated by on shaker. The solution was separated from conical flasks at intervals of time and analyzed for the uptake of chromium(VI). The kinetics of chromium(VI) adsorption on adsorbents were analyzed using pseudo first-order and pseudo second-order kinetic models. A relatively high R^2 value indicates that the model successfully describes the kinetics of Cr(VI) adsorption.

2.3.1. First-order rate kinetics
It is generally expressed as follows

$$\frac{dq_t}{dt} = k_1(q_e - q_t) \tag{5}$$

where q_e and q_t are the adsorption capacities at equilibrium and at time t, respectively (mg/g), k_1 is the rate constant of pseudo first-order adsorption (min^{-1}).

After integration and applying boundary conditions $t = 0$ and $t = t$ and $q_t = 0$ and $q_t = q_e$ the integrated form of Eq. (5) becomes:

$$\log(q_e - q_t) = \log(q_e) - \frac{k_1}{2.303}(t). \tag{6}$$

2.3.2. Second-order rate kinetics
The pseudo second-order adsorption kinetic rate equation is expressed as:

$$\frac{dq_t}{dt} = k_2(q_e - q_t)^2 \tag{7}$$

where k_2 is the rate constant of pseudo second-order adsorption (g mg^{-1} min^{-1}).

For the boundary conditions $t = 0$ and $t = t$ and $q_t = 0$ and $q_t = q_e$ the integrated form of Eq. (7) becomes:

$$\frac{1}{q_e - q_t} = \frac{1}{q_e} + k_2 t \tag{8}$$

which is the integrated rate law for pseudo second-order reaction. Eq. (8) can be rearranged to obtain (9), which has a linear form:

$$\frac{t}{q_t} = \frac{1}{k_2 q_e^2} + \frac{1}{q_e}(t) \tag{9}$$

2.4. Column adsorption studies

Adsorbent is packed in a column reactor and almost no flow or movement of adsorbent is taking place inside the column. Fixed bed adsorption studies were conducted to evaluate dynamic behavior for Cr(VI) removal on adsorbents. The experimental set-up consisted of glass column (3.0 cm ID, 30.0 cm length) packed with different bed heights of adsorbent. Sample feed flow rate was varied and maintained throughout the experiments. At the exit of the column, flow rate was also measured so as to get steady state flow conditions in the column. Experiments were conducted at optimum pH 3, determined from batch experiments [31].

Effect of inlet feed flow rate, initial adsorbate concentration (10–30 mg/L) and adsorbent bed height (1.5–5.0 cm) were investigated on the performance of breakthrough for the adsorption of Cr(VI).

2.5. Characterization of the products

Chemical characterization of product and spent adsorbent explored to understand the mechanism of the process involved application of Scanning electron microscopy (SEM), Energy dispersive X-ray analysis (EDX) and Fourier transformed infra-red spectroscopy (FTIR).

Surface morphology of the adsorbents was visualized on SEM (model LEO 440, LEO Electron Microscopy Ltd, Cambridge, England). EDX analysis is used for identifying the elemental composition of a specimen. EDX (model 7060, Oxford Instruments, UK) analysis system works as an integrated feature of a SEM and cannot operate on its own without the latter.

The presence of functional groups in the adsorbents was confirmed by FTIR analysis. FTIR spectra of native and chromium-loaded adsorbents were recorded on PerkinElmer-RX1 and FTIR 8201 Shimadzu spectrometers. The spectra of adsorbents were measured within the range of 500–4000 cm^{-1} wave number. The spectra were plotted using the same scale on the transmittance axis for adsorbent before and after adsorption of chromium were used to determine the vibrational frequency changes in the functional groups of adsorbent. The spectra display a number of absorption peaks, indicating the complex nature of the examined adsorbent, and the binding of chromium with functional groups present in the adsorbent.

2.6. Safety evaluation of the adsorbents by ecotoxicological assessment

Adult freshwater teleosts *Poecilia reticulata* (guppy fish) were procured locally and acclimatized under standard laboratory conditions. For safety evaluation of the adsorbents a limit test was performed. The 96 h static acute toxicity test was conducted [32]. Each glass aquaria containing 12 fish were exposed to 0.1 g/L of adsorbents used. Experiment on control group of fish was conducted in parallel. The fish were not fed 24 h before and during the tests. Precautions were taken to remove the dead fish and debris from the aquaria immediately.

The physicochemical properties of the tap water used in the experiment were temperature (22.4 ± 1.6 °C), pH (7.2 ± 0.02), dissolved oxygen (6.8 ± 0.4 mg/L), alkalinity (95 ± 100 mg/L) and hardness (118 ± 12.2 mg/L as calcium carbonate).
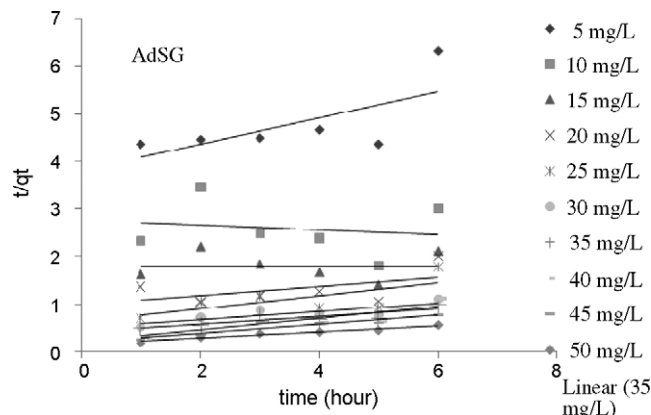
3. Results and discussion

3.1. Thermodynamics

The value of K_c for AdSG was 5.69 at temperature 303 K. The corresponding $\Delta G°$ value was −4.4 kJ mol^{-1}. The values of standard enthalpy change ($\Delta H°$) and standard entropy change ($\Delta S°$) were found out to be as 0.46 kJ mol^{-1} and 1.68 J mol^{-1} K^{-1} respectively (Table 1).

A positive value of $\Delta H°$ as 0.46 kJ mol^{-1} for chromium removal with AdSG indicated the endothermic nature of the process. A negative value of the free energy of AdSG ($\Delta G°$) (−4.4 kJ mol^{-1} at 303 K), indicated spontaneous nature of the adsorption process. It was also noted that the change in free energy, increases with increase in

Fig. 1. Pseudo first-order kinetic parameters for the adsorption of chromium(VI) on AdSG.

Table 2
Pseudo first-order kinetic parameters for the adsorption of Cr(VI) on AdSG.

Cr(VI) Concentration (mg/L)	k_1 (min^{-1})	q_e (equation)	q_e (plot)	R^2
5	−0.0094	1.15	1.04	0.339
10	−0.2372	2.76	3.13	0.969
15	−0.2948	3.61	4.38	0.973
20	−0.2165	4.76	4.29	0.702
25	0.2303	5.41	3.33	0.522
30	−0.3339	6.62	6.90	0.901
35	−0.3616	7.15	7.28	0.905
40	−0.5665	7.98	1.81	0.408
45	−0.3731	8.54	6.95	0.897
50	−0.5021	11.4	11.83	0.968

temperature, which exhibits an increase in adsorption with rise in temperature. This could be possibly because of activation of more sites on the surface of AdSG with increase in temperature. A positive value of $\Delta S°$ as 1.68 J mol^{-1} K^{-1} for AdSG showed increased randomness at solid solution interface during the adsorption of Cr(VI) on adsorbents.

3.2. Kinetic study

Adsorption kinetic study describes the solute on the activated carbons, i.e. the adsorption mechanism was analyzed using pseudo first-order [33] and pseudo second-order [34] kinetic models.

3.2.1. First-order rate kinetics

First-order equation of Lagergren did not apply throughout the complete range of contact time. Plots of log($q_e - q_t$) versus time for AdSG deviated considerably from the experimental data after a short period (Fig. 1). The slopes and intercepts as calculated from the plots were used to determine k_1 (first-order rate constant) and q_e (equilibrium capacity). The q_e values for AdSG as calculated from the first-order rate equation are approximately equal to the experimental values of k_1 and q_e together with their regression coefficients (Table 2). Therefore, it can be concluded that in case of AdSG chromium–adsorbent systems, follow a first-order rate equation.
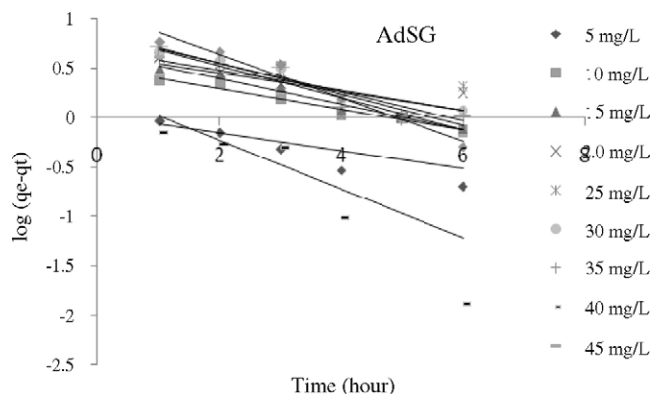
Table 1
Thermodynamic parameters of AdSG.

R (kJ mol^{-1} K^{-1})	T (K)	K_c	ΔG (kJ mol^{-1})	ΔH (kJ mol^{-1})	ΔS (kJ mol^{-1} K^{-1})	R^2
8.3×10^{-3}	303	5.69	−4.38	0.46	1.68	0.99
8.3×10^{-3}	313	5.99	−4.66			
8.3×10^{-3}	323	6.39	−4.97			

Fig. 2. Pseudo second-order kinetic parameters for the adsorption of chromium(VI) on AdSG.

3.2.2. Second-order rate kinetics

The plot of (t/q_e) and t of Eq. (8) should give a linear relationship from which q_e and k_2 can be determined from the slope and intercept of the plot, respectively (Fig. 2). The correlation coefficients (R^2) for the linear plots are not superior in the case of AdSG. The values of q_e and k_2 are presented in Table 3.

3.3. Column adsorption studies

Fixed bed column adsorption experiments were carried out to study the adsorption dynamics. Experimental data of batch studies are difficult to apply directly to column adsorber because isotherms are unable to give accurate data for scale up since a flow column is not at equilibrium. This operation allows more efficient utilization of the adsorptive capacity than the batch experiment results. The adsorbent is contacted continuously by the solution at the initial solute concentration. All the fixed bed column experiments were carried out at optimum adsorbent bed height, flow rate, initial chromium concentration and pH 3 having Cr(VI) concentration as 10 mg/L. Flow rate of the sample through the column was maintained at 4 mL/min. Breakthrough volumes obtained at bed heights of 1.5 cm, 3.0 cm and 5 cm for sample having Cr(VI) concentration as 10 mg/L and pH 3 were found out to be 7.40×10^3 mL, 9.80×10^3 mL and 1.12×10^4 mL for AdSG respectively. The total chromium adsorbed in the column for a given feed concentration is equal to the area under the breakthrough curve. Breakthrough curve steepness was a strong function of column parameters.

3.3.1. Effect of column height

Chromium solution was passed through the fixed bed column having Cr(VI) concentration as 10 mg/L with pH 3 (without changing the pH). The performance of breakthrough curves at a bed height of 1.5 cm, 3.0 cm and 5.0 cm for AdSG (Fig. 3). It

Table 3
Pseudo second-order kinetic parameters for the adsorption of chromium(VI) on AdSG.

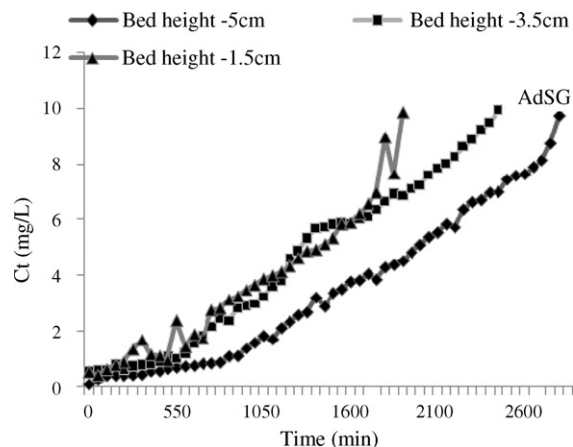| Cr(VI) Conc. (mg/L)	k_2 (g mg^{-1} min^{-1})	q_e (equation)	q_e (plot)	R^2
5	4.09	1.15	0.26	0.457
10	−0.01	2.76	−3.65	0.023
15	−0.01	3.61	−0.55	0.012
20	0.09	4.76	1.03	0.251
25	0.05	5.41	1.61	0.461
30	0.02	6.62	2.04	0.683
35	0.02	7.15	2.42	0.764
40	0.01	7.98	4.85	0.798
45	0.01	8.54	5.52	0.856
50	0.01	11.4	15.15	0.951

Fig. 3. Effect of bed height in column study for AdSG.

is evident from these curves that an increase in column depth increases throughout the volume treated due to higher contact time. At relatively lower contact time, the curve was steeper for both the samples showing the faster exhaustion of the bed. For Cr(VI) removal the treated volume varied from 7.40×10^3 mL to 1.12×10^4 mL for AdSG as the bed height was increased from 1.5 cm to 5.0 cm (Fig. 3). Increase in the metal uptake capacity with the increase of bed height in the fixed bed column was probably due to increased surface area of the adsorbent, which provide more binding sites for the adsorption. The breakthrough time was also increased with the increase of bed height (Table 4).

The varying degrees of chromium uptake efficiencies observed for the same quantity of adsorbents packed in different length/diameter patterns and operated under identical conditions could be explained as follows. When chromium solution is passed through bed of adsorbent, most of the adsorbate is initially adsorbed at the inlet part of the bed, building up of a saturated zone. As more liquid is passed the saturated zone moves forward until the breakthrough is reached. The adsorption capacities of the columns with three different bed heights were in order of 1015.5 (longer bed), 532.5 (medium bed depth) and 365.1 (shorter bed depth) in case of AdSG (Table 4).

3.3.2. Effect of flow rate

The effect of flow rate on breakthrough performance, at a bed height of 1.5 cm was shown. As can be seen from the breakthrough plots, higher efficiency of the process for AdSG at lower flow rate (Fig. 4). These breakthrough curves demonstrate influence of
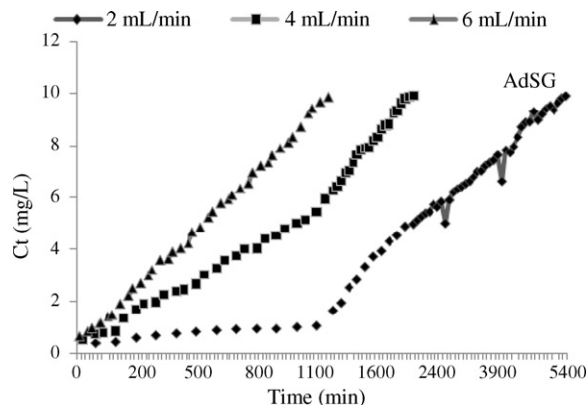

Fig. 4. Effect of flow rate in column study for AdSG.

Table 4
At different column depth for AdSG.

Column diameter (cm)	Column height (cm)	Time to attain equilibrium (min)	Effluent volume (mL)	Total adsorption (mg/bed)	Maximum uptake (mg/g)
1.65	5.0	2800	11200	3046.4	1015.5
2.20	3.0	2450	9800	1597.4	532.5
3.00	1.5	1900	7400	1095.2	365.1

adsorption kinetics. The flow rate was varied from 2 mL/min to 6 mL/min while the inlet Cr(VI) concentration was kept constant at 10 mg/L at pH 3. The uptake of chromium decreased with increase in flow rate. It was also observed that adsorbents get saturated easily at higher flow rates. As volumetric flow rate increases, the velocity through bed decreases, which results in decrease in the length of adsorption zone. At higher flow rates breakthrough curves become steeper with decrease in breakpoint time and the adsorbed ion concentration decreases. A higher chromium uptake was observed at the beginning of fixed bed column operation but as solution continued to flow, the concentration of chromium in the sample rapidly increased. The bed becomes saturated with chromium and solute concentration in the sample rise sharply.

An increase in flow rate from 2 mL/min to 6 mL/min reduced the volume of sample treated from 1.60×10^4 mL to 4.75×10^3 mL for Cr(VI) removal for AdSG. As Cr(VI) ions move from bulk solution to the surface of film surrounding the adsorbent particle. Concentration gradient was developed at the interface, which allows the solute particles to penetrate through the film, and reach the surface of particles where the positively active sites attract the negatively charged dichromate ions. At higher flow rates, film surrounding the particle breaks, thereby reducing the adhesion of adsorbate to adsorbent particle. As can be seen from chromium uptake of AdSG decreased with increase in flow rate (Fig. 4). The breakthrough capacity of adsorbents decreased with increase in flow rate. As the flow rate through the bed decreased, the depth of adsorption zone decreased because of more time for adsorption. The adsorption capacity of the bed column decreased with increasing flow rate of the adsorbate solution. The maximum adsorption efficiency achieved was 1632 mg Cr/adsorbent bed of AdSG, at the lowest flow rate of 2 mL/min (Table 5).

At higher flow rates, the retention period of Cr(VI) ions in the adsorption column was too short and the metal ions did not have sufficient time to diffuse into the metal binding sites of the porous beds. However, at lower flow rates (i.e., higher retention period), the diffusion of Cr ions to the active adsorbing sites is more efficient and permitted more effective mass transfer rates under such conditions. The total uptake capacities at low (2 mL/min), medium (4 mL/min) and high (6 mL/min) flow rates of the feed solution were in the order 544.0 > 365.1 > 256.6 in case of AdSG (Table 5). Depending on differences in flow rates and retention time, the breakpoint time also exhibited variations. Column experiments at highest flow rate attained breakthrough more quickly (792 min) than that at moderate (1850 min) and lowest flow rates (8000 min) for AdSG. Therefore, the volume of sample that can be treated is a function of both the concentrations of metal contaminant present in sample as well as hydraulic retention time.

Fig. 5. Effect of inlet concentration in column study by AdSG.

3.3.3. Effect of initial chromium concentration

Effect of initial chromium concentration on the performance of breakthrough curve was observed. Breakthrough volume obtained at bed height of 1.5 cm, samples having flow rate as 4 mL/min through the bed and having Cr(VI) concentration as 10 mg/L Cr(VI) for AdSG at pH 3 was 7.40×10^3 mL (Fig. 5). A change in the inlet adsorbate concentration affected the operating characteristics of the fixed bed column. At low initial concentration, delayed breakthrough occurred and the treated volume was higher since the lower concentration gradient caused a slower transport due to decreased mass transfer coefficient [35]. This could be due to increase in number of binding sites. The adsorbent gets saturated early at high initial concentration because binding sites become more quickly saturated in the system. These results indicated that increase in chromium concentration reduced the metal to adsorbent ratio, and the metal uptake as long as the adsorbent was not saturated. Initial adsorbate concentration affected the performance of fixed bed for adsorption of chromium (Fig. 5). Breakpoint time decreased with increasing inlet Cr(VI) concentration as the binding sites were saturated faster. These results showed that performance of breakthrough curves for chromium removal by AdSG was strongly affected by initial concentration and thus, affected the treatment of samples.

The maximum uptake capacity of 150.67 mg/g for AdSG had been attained for the feed solution of highest concentration (Table 6). For all metal concentrations, the flow rate, bed depth and column size were kept uniform in all experiments. The only variable here is the number of Cr ions passing through the column when different concentrations of solutions were passed through the packed bed. At higher inlet concentrations, the number of ions competing for binding sites is more and causes greater resistance to the mass

Table 5
Influence of flow rate on Cr(VI) uptake for AdSG.

Flow rate (mL/min)	Time to attain equilibrium (min)	Effluent volume (mL)	Total adsorption (mg/bed)	Maximum uptake (mg/g)
2	8000	16000	1632	544.0
4	1850	7400	1095.2	365.1
6	792	4752	769.8	256.6

Table 6
At different inlet Cr(VI) concentration for AdSG.

| Inlet Cr(VI) Concentration	Time to attain equilibrium (min)	Effluent volume (mL)	Total adsorption (mg/bed)	Maximum uptake (mg/g)
10	1850	7400	1095.2	365.1
20	1300	5200	717.6	239.2
30	1000	4000	452	150.7

transfer of metal ions to the bed column. Therefore, the percentage of adsorption decreases at higher concentration of feed solution. The quantity of Cr(VI) ions removed by the packed bed column for varying inlet concentrations was in order of 365.1 (10 mg/L) < 239.2 (20 mg/L) < 150.7 (30 mg/L) for AdSG.

### 3.4. Characterizations and mechanism of chromium adsorption

Maximum Cr(VI) adsorption over AdSG is above 90% at initial pH 3.0. To determine the behavior of adsorbent towards adsorption of Cr(VI), scanning electron microscopy (SEM), electron dispersive X-ray (EDX) and Fourier transform infra red spectroscopy (FTIR) were carried out on AdSG before and after chromium removal. The results explained the mechanism for chromium uptake by AdSG at low pH. SEM of AdSG adsorbent exhibited the fibrous nature of adsorbent (AdSG) saturated with chromium. SEM of AdSG before and after saturation with Cr(VI) showed no change in the structure of AdSG (Figs. 6 and 7).

EDX study reveals that chromium ions were present in the treated samples but not in the untreated one. It clearly indicates the adsorption of chromium on the surface of the adsorbents (Figs. 8 and 9). EDX analysis provides direct evidence that chromium is superficially adsorbed on AdSG, thus the removal may not be due to adsorption but simply surface precipitation. Thus, this analysis provides the direct evidence for the specific adsorption of chromium on the surface of above-mentioned adsorbents.

FTIR of AdSG before and after saturation with Cr(VI) was carried out to identify the functional group effective for adsorption. IR wavelength used in this study was in the range of 2.5–15 μm. Functional groups involved in the removal of chromium were identified by analysis of IR spectrum of AdSG before and after saturation with Cr(VI) (Figs. 10 and 11). The FTIR bands observed at wave numbers 2933.6 cm^{-1}, 2134.9 cm^{-1}, 1757.8 cm^{-1}, 1658.3 cm^{-1} and 718.6 cm^{-1} with fresh adsorbents were found missing with AdSG saturated with Cr(VI) ions. These results indicated that these bonds
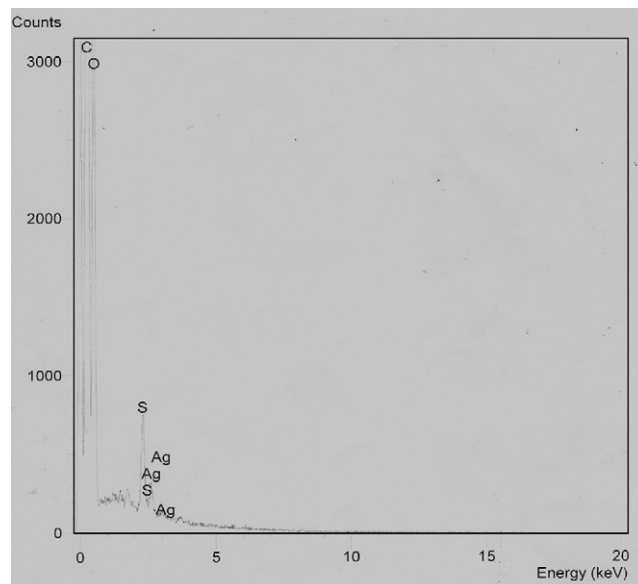

Fig. 7. Electron dispersive X-ray analysis of AdSG.

were involved with adsorption of Cr ions. In case of AdSG, the bond involved in adsorption at the wave numbers 2933.6 cm^{-1} is a broad peak showing the presence of carboxylic group. Where as the bonds found missing at wave number 2134.9 cm^{-1}, 1757.8 cm^{-1} and 1658.3 cm^{-1} shows presence of symmetrical alkyne, a ketonic group specially anhydride and unsymmetrical alkenes as well as amide ($-CONH_2$) bonds, respectively. The band missing at 718.6 cm^{-1} shows NH_2 and N–H bonds which shifted on H-bonding. At low pH (pH ≤ 3) all the chromium complexes exist as negatively charged dichromate ions ($HCr_2O_7^-$). Further, the concentration of hydronium ion is large at low pH. Due to electromeric effect, the sites become positively charged and the number of sites
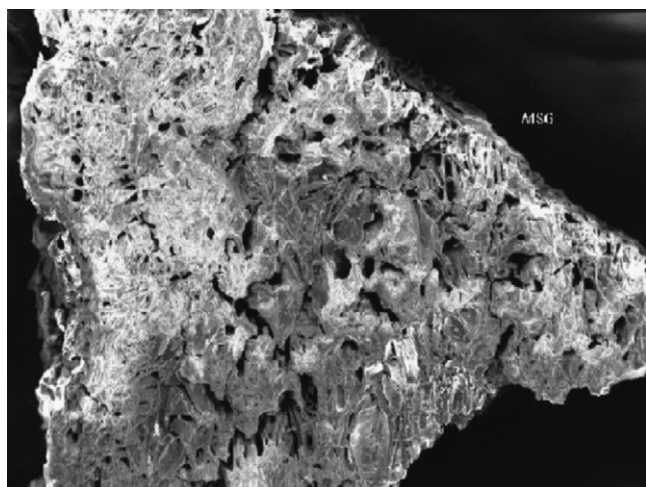
Fig. 6. Scanning electron microscope of AdSG.
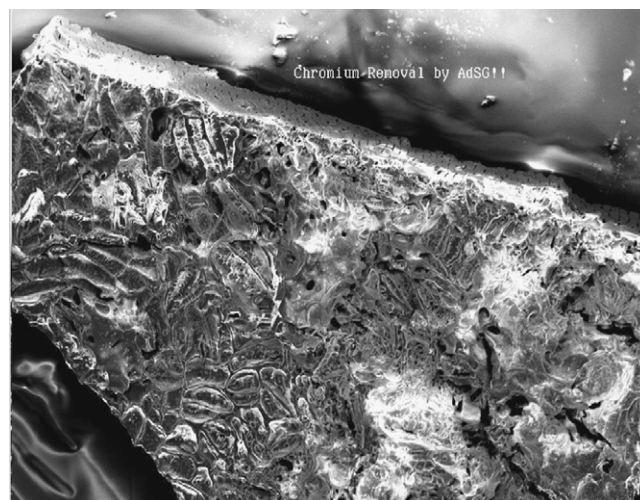
Fig. 8. Scanning electron microscope of AdSG + chromium.

Table 7
Test observations.

| Treatment	No. of fish	Average body weight (g)		% Variation in body weight	Mortality
		Initial	Final		
Control	12	0.4	0.4	Nil	0/12
Exposed (0.1 g/L)	12	0.5	0.5	Nil	0/12
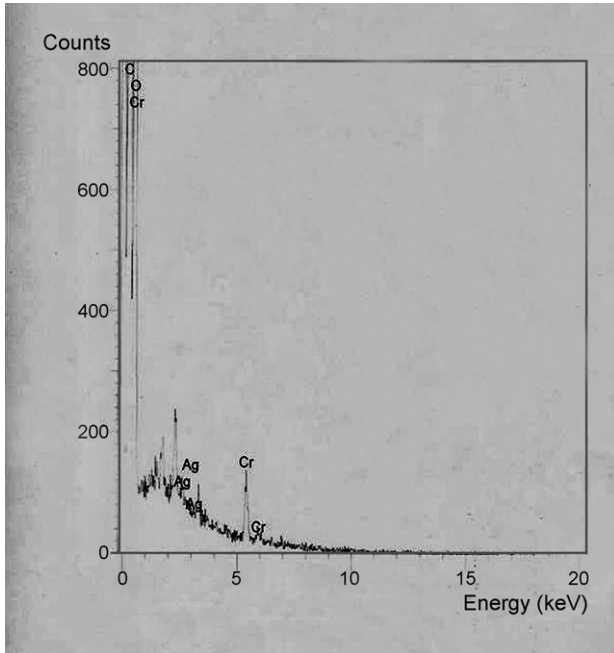
Fig. 9. EDX analysis of AdSG + chromium.

increases, thereby attracting negatively charged dichromate ions. This phenomenon results into high and selective removal of Cr(VI) at low pH. Removal of toxic hexavalent form of chromium from solutions was possible using selected adsorbents.

Moreover, the peak intensity of the carbonyl group was greatly decreased and shifted from 1853.3 cm^{-1} to 1813.3 cm^{-1}. Therefore, it can be suggested that the carbonyl and hydroxy groups from the
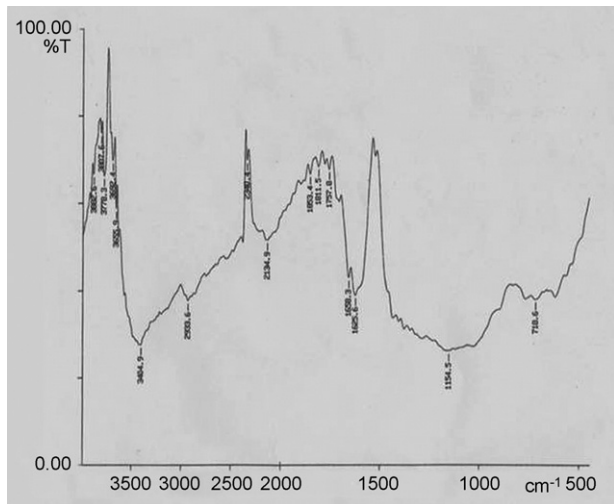
Fig. 10. FTIR analysis of AdSG.
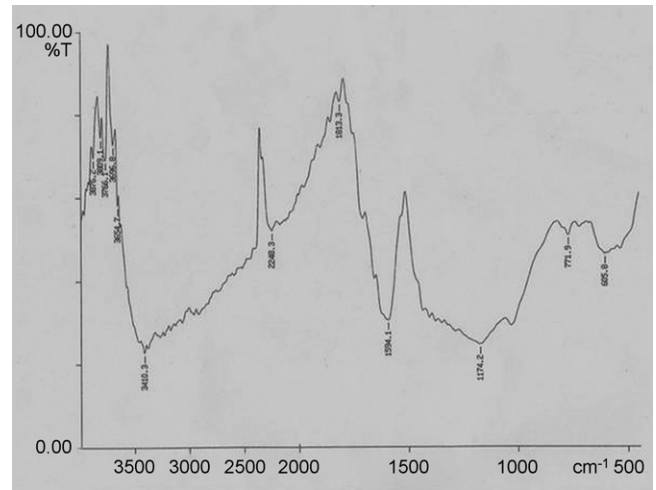
Fig. 11. FTIR analysis of AdSG.

structures of AdSG adsorbent may be involved in the mechanism of chromium adsorption.

3.5. Safety evaluation of adsorbent by ecotoxicological assessment

Bioassay test were conducted for the safety evaluation of these adsorbents using standard test fish *Poecelia reticulata* (guppy) as per guidelines [32]. Acclimatized guppy fish (10 days) was exposed to the treated adsorbent AdSG for the period of 96 h in glass aquaria under the static laboratory conditions. It is noticed that there is no loss of positive rheotaxis and behavior of fish during the exposure. Survival of test fish was recorded 100% after 96 (Table 7). This adsorbent is safe for the aquatic ecosystem in particular and total environment, in general along with human health.

There was no mortality recorded in fish exposed to test material and variation in body weight was observed in exposed fish, and the test material is non-toxic to fish. Therefore it is concluded that adsorbents screened are suitable for the removal of chromium(VI) from water.

Acknowledgments

References

[1] S.Y. Quek, D.A.J. Wase, C.F. Forster, The use of sago waste for the sorption of lead and copper, Water S. A. 24 (1998) 251–256.
[2] M.A. Armienta-Hernnandez, R. Rodriguez-Castillo, Environmental exposure to chromium compounds in the valley of Leon, Mexico, Environ. Health Perspect. 103 (1995) 47–51.

[3] R. Schmuhl, H.M. Krieg, K.A. Keizer, Adsorption of Cu(II) and Cr(VI) ions by chitosan: kinetics and equilibrium studies, Water S. A. 27 (2001) 1–7.
[4] V. Hassmanova, J. Vaneckova, K. Bousova, Occupational diseases caused by chromium and its compounds, Acta Med. (Hradec Kralove) Suppl. 43 (2000) 33–36.
[5] L. Kanerva, R. Jolanki, T. Estlander, K. Alanko, A. Savela, Incidence rates of occupational allergic contact dermatitis caused by metals, Am. J. Contact Dermat. 11 (2000) 155–160.
[6] D.G. Barceloux, Chromium, J. Toxicol. Clin. Toxicol. 37 (1999) 173–194.
[7] EPA (Environmental Protection Agency) Environmental Pollution Control Alterations, 1990, EPA/625/5-90/025, EPA/625/4-89/023, Cinacinnati, US.
[8] E. Cooney, B. Luo, J.W. Patterson, C. Petropoulou, Toxicity reduction methodologies, in: D.L. Ford (Ed.), Water Quality Management Library, vol. 3, Technomic, Lancaster, PA, 1992, pp. 109–181.
[9] J.A.S. Tenorio, D.C.R. Espinosa, Treatment of chromium plating process effluents with ion exchange resins, Waste Manage. 21 (2001) 637–642.
[10] A. Alliane, N. Bounatiro, A.T. Cherif, D.E. Akretche, Removal of chromium from aqueous solution by complexation-ultrafiltration using a water-soluble macro ligand, Water Res. 35 (2001) 2320–2326.
[11] A.Lj. Bojic, M. Purenovic, D. Bojic, Removal of chromium (VI) from water by micro-alloyed aluminium composite (MAlC) under flow conditions, Water S.A. 30 (2004) 353–360.
[12] S. Chunming, L.D. Ralph, Treatment of hexavalent chromium in chromite ore processing solid waste using a mixed reductant solution of ferrous sulfate and sodium dithionite, Environ. Sci. Technol. 39 (2005) 6208–6216.
[13] N. Kongsricharoern, Application of electrochemical precipitation of treatment of Cr wastewater, Doctoral Thesis, Asian Institute of Technology, Bangkok, 1994.
[14] S. Rengaraj, K.H. Yeon, S.H. Moon, Removal of chromium from water and wastewater by ion exchange resins, J. Hazard. Mater. 87 (2001) 273–287.
[15] L. Yurlova, A. Kryvoruchko, Removal of Ni (II) ions from wastewater by micellar-enhanced ultrafiltration, Desalination 144 (2002) 255–260.
[16] Y. Benito, M.L. Ruiz, Reverse osmosis applied to metal finishing wastewater, Desalination 142 (2002) 229–234.
[17] J.L. Bersillon, Water purification and disinfection processes, Acta Hydrochem. Hydrobiol. 27 (1999) 98–100.
[18] N.K. Lazaridis, D.D. Asouhidou, Kinetics of sorptive removal of chromium (VI) from aqueous solutions by calcined Mg–Al–CO$_3$ hydrotalcite, Water Res. 37 (2003 2875).
[19] M. Kobya, Adsorption, kinetic and equilibrium studies of Cr (VI) by hazelnut shell activated carbon, Adsorp. Sci. Technol. 22 (2004) 51–64.
[20] S. Babel, T.A. Kurniawan, Cr (VI) removal from synthetic wastewater using coconut shell charcoal and commercial activated carbon modified with oxidizing agents and/or chitosan, Chemosphere 54 (2004) 951–967.
[21] N.R. Bishnoi, M. Bajaj, N. Sharma, A. Gupta, Adsorption of Cr (VI) on activated rice husk carbon and activated alumina, Bioresour. Technol. 91 (2004) 305–307.
[22] S.R. Bai, T.E. Abraham, Continuous adsorption and recovery of Cr (VI) in different types of reactors, Biotechnol. Prog. 21 (2005) 1692–1699.
[23] D. Parka, Y.S. Yunb, J.M. Parka, Studies on hexavalent chromium biosorption by chemically-treated biomass of *Ecklonia* sp, Chemosphere 60 (2005) 1356–1364.
[24] K.M.S. Sumathi, S. Mahimairaja, R. Naidu, Use of low-cost biological wastes and vermiculite for removal of chromium from tannery effluent, Bioresour. Technol. 96 (2005) 309–316.
[25] F.N. Saifuddin, P. Kumaran, Removal of heavy metals from industrial wastewater using chitosan coated oil palm shell charcoal, Electron. J. Biotechnol. 8 (2005) 43–53.
[26] V. Campos, P.M. Buchler, Removal of chromate from drinking water using powder carbon steel, Environ. Geol. 47 (2005) 926–930.
[27] V. Sarin, K.K. Pant, Removal of chromium from industrial waste by using eucalyptus bark, Bioresour. Technol. 97 (2006) 15–20.
[28] M.S. Gasser, G.H.A. Morad, H.F. Aly, Batch kinetics and thermodynamics of chromium ions removal from waste solutions using synthetic adsorbents, J. Hazard. Mater. 142 (2007) 118–129.
[29] K. Perisamy, K. Srinivasan, P.K. Murugan, Studies on Cr (VI) removal by activated groundnut husk carbon, Ind. J. Environ. Health 33 (1991) 433–439.
[30] W.T. Tan, S.T. Ooi, C.K. Lee, Removal of Cr (VI) from solution by coconut husk and palm pressed fibers, Environ. Technol. 14 (1993) 277–282.
[31] S.P. Dubey, K. Gopal, Adsorption of chromium (VI) on low cost adsorbents derived from agricultural waste material: a comparative study, J. Hazard. Mater. 145 (2007) 465–470.
[32] Organization for Economic Co-operation and Development: Test Guideline 404, OECD Guideline for Testing of Chemicals, Washington, DC, 2004.
[33] S. Lagergren, Zur theorie der sogenannten adsorption geloster stoffe. Kungliga Svenska Ventenskspsakademiens, Handlingar 24 (1990) 1–39.
[34] Y.S. Ho, G. McKay, D.A.J. Wase, C.F. Foster, Study of the sorption of divalent metal ions on to peat, Adsorp. Sci. Technol. 18 (2000) 639–650.
[35] Z. Aksu, G.F. Ferda, Biosorption of phenol by immobilized activated sludge in a continuous packed bed: prediction of breakthrough curves, Process Biochem. 39 (2004) 599–613.